THE ASTROPHYSICAL JOURNAL, 241:811–819, 1980 October 15

THE ROTATION OF THE SUN: OBSERVATIONS AT STANFORD

PHILIP H. SCHERRER, JOHN M. WILCOX, AND LEIF SVALGAARD[1]
Institute for Plasma Research, Stanford University
Received 1980 February 11; accepted 1980 April 11

ABSTRACT

Daily observations of the photospheric rotation rate using the Doppler effect have been made at the Stanford Solar Observatory since 1976 May. These observations show no daily or long-period variations in the rotation rate that exceed the observational error of about 1%. The average rotation rate is the same as that of the sunspots and the large-scale magnetic field structures.

Subject headings: Sun: rotation

I. INTRODUCTION

Measurements of the photospheric rotation rate using the Doppler effect have been the subject of controversy ever since they were first made (e.g., Plaskett 1915; DeLury 1939; Hart 1954; Howard and Harvey 1970; and Plaskett 1973) and have been recently reviewed by Howard (1978). Daily observations at the Stanford Solar Observatory (SSO) have been made since 1976 May. Analysis of the 731 full-disk low-resolution Dopplergrams made to date yields results that conflict with some other recent sets of observations. The SSO observations show no daily or long-period variations in the rotation rate that exceed observational error, and the average rate is about the same as that of the large-scale magnetic field structures and sunspots. These conclusions are apparently inconsistent with the well-known results of Howard and Harvey (1970).

II. MEASUREMENT OF SOLAR ROTATION

The SSO instrument design is very similar to the solar magnetograph at the Mount Wilson 150 foot tower telescope (Howard, Tanenbaum, and Wilcox 1968; Howard and Harvey 1970; and Howard 1976*a*) but was designed for only low spatial resolution observations. Since some of the differences may affect rotation measurements, the relevant details will be described. The overall design philosophy of the SSO has been described by Scherrer *et al.* (1977). Preliminary rotation results and the modification to the instrument to allow full-disk 3′ magnetograms and Dopplergrams are described by Duvall (1979). Svalgaard, Scherrer, and Wilcox (1979) made a preliminary report of the conclusions to be described more fully in this paper. The results presented here differ slightly from the two earlier reports due to recalibration of the position, intensity, and velocity data. The calibration methods used in the present work are described below.

a) Position Calibration

The SSO telescope is outlined in Figure 1. The instrument consists of a vertical telescope with focal length of 6.5 m feeding a vertical 22.8 m Littrow spectrograph. The spectrograph is used in the 5th order with a reciprocal dispersion of 12.9 mm $Å^{-1}$ at 5250 Å. The entrance aperture consists of a 6 mm square mask, an image slicer, and a 0.75 mm × 100 mm slit. There are several systematic effects that must be examined when using this entrance aperture arrangement for low-resolution observations. These influence the effective position of the aperture on the Sun and the measured velocity.

The scanning system used is similar to most magnetograph instruments. A limb guider controls the orientation of the second-flat mirror with an analog servo system. The guider image is produced by an auxiliary lens with focal length of 7.0 m. The Sun is scanned by moving the guider north-south and east-west in steps of 0.001 inch. The position angle of the solar pole relative to the scanning axes is computed from the date and location of the coelostat mirror. The magnetogram/Dopplergram scan is made by stepping the image to fixed positions and integrating for 15 s at each location, instead of with a continuous motion. The scan is made in east-west lines (on the Sun) stepping 90″ between integrations with 180″ between lines. The aperture is 180″ square and is oriented parallel to the entrance slit which is north-south in the room. Prior to 1978 February 15 the aperture was rotated to be parallel to central meridian on the image, resulting in non-uniform illumination of some of the image slicer segments. Although no difference in the velocity data

[1]Now at Universite de Liège, Institut d'Astrophysique, Cointe-Ougrée, Belgium.

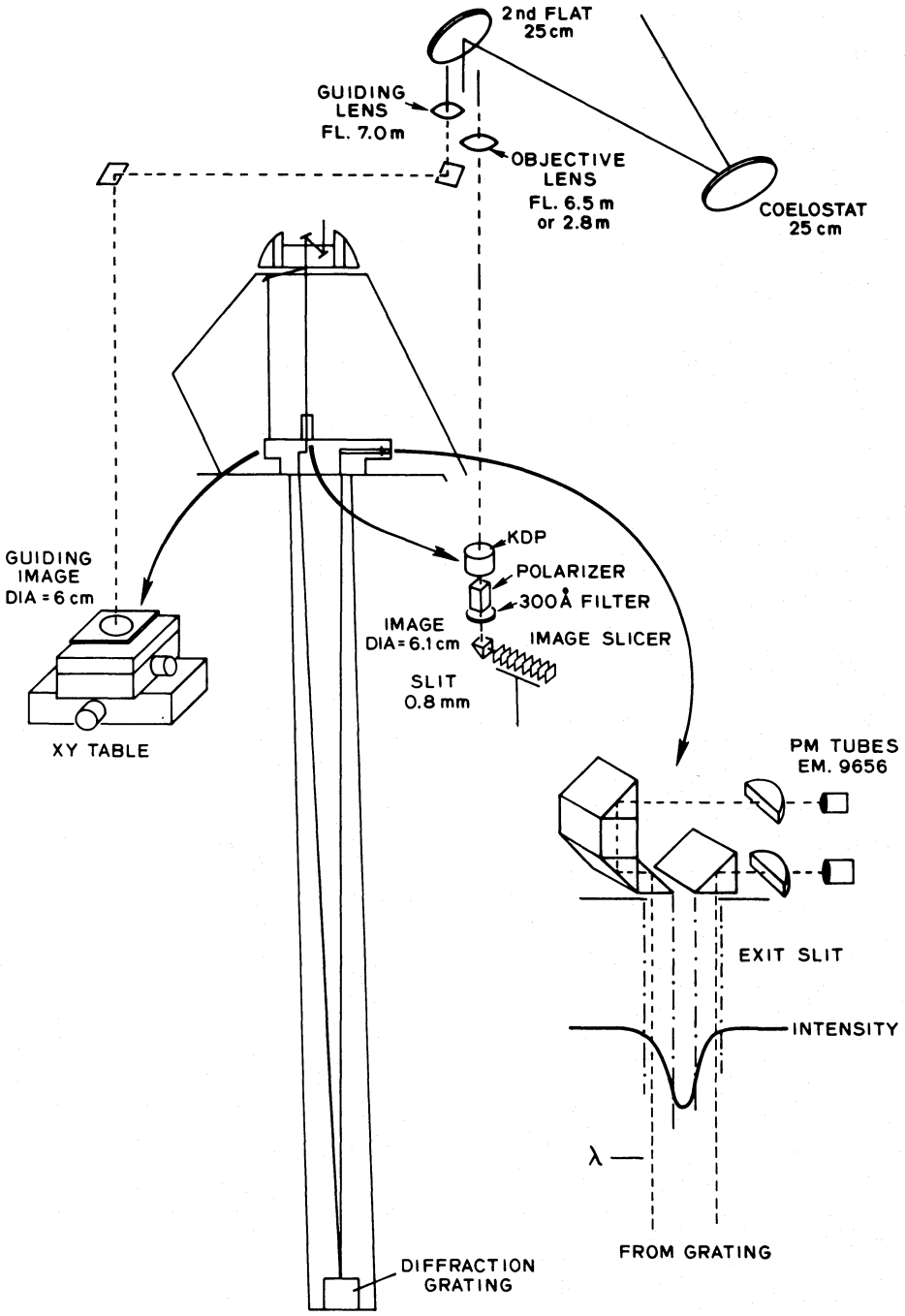

FIG. 1.—A schematic diagram of the Stanford Solar Telescope. Note the separate light path for the guider image and the observing image. The actual distance between the guider lens and the guider photodiodes is used to define the telescope scale. The spectrograph head is at ground level with the Littrow lens and diffraction grating at the bottom of a 23 m pit.

was found for several pairs of observations with the aperture oriented each way, there is less risk of systematic errors with the present alignment.

In order to measure solar rotation the conversion between scanner coordinates and effective heliocentric coordinates must be accurate. The telescope scale is defined by the 6.97 m distance between the guiding lens and the scanning table. The angular size of the solar disk is computed for the day of observation, and the geometrical position on the disk is found for each scanner position. If the observing aperture were only a few arcsec wide this would be sufficient to define the

heliocentric position; however, with a 180″ aperture the limb darkening across the aperture will weight the effective position of the aperture toward the center of the disk. An effective position is computed for each actual aperture position using the average observed limb-darkening function. For the aperture position at the limb, the correction is about a third the aperture size. The correction decreases rapidly away from the limb. For the rotation analysis described below, only the center half of the area of the disk is used, i.e., only points within 0.75 of a radius of the center of the disk. The maximum position correction for the points used is 4″. If the correction were omitted from the rotation analysis the computed equatorial rotation rate would be 0.25% too low (about 5 m s^{-1}).

b) *Intensity Calibration*

As part of normal magnetograph operation the brightness of the image is recorded during each integration. This is primarily used to compensate the magnetic field signal for brightness fluctuations. For each scan the individual intensity measurements are corrected for limb darkening and averaged over the center half of the disk. The variance of this quantity is used as a part of a quality figure for the scan. The magnitude of the average intensity will depend on the zenith angle, the photomultiplier tube voltage, the sky quality, and the cleanliness of the optics. Since the phototube voltages are rarely changed (twice per year) this quantity can be used to monitor the cleanliness of the sky and optics. When it was discovered that the average intensity could also be used to compute a correction for the effect of scattered light on the velocity observations, an effort was made to calibrate the intensity for the phototube voltages used since the start of the observations.

When the telescope is not making a magnetogram or some special observation, it is used for mean solar magnetic field observations. There are therefore several measures of the intensity of integrated sunlight for each day. All of the intensity observations for each day were plotted on a log scale as a function of computed air mass. A typical plot is shown in Figure 2. It can be seen that the expected linear relationship is found. The intercept corresponds to the intensity that would have been observed without the intervening atmosphere.

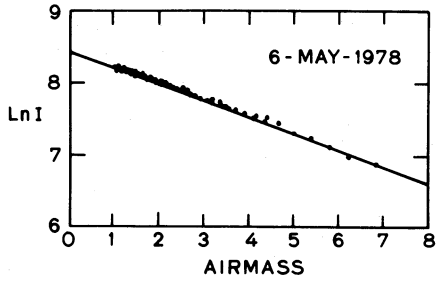

FIG. 2.—The change in observed image brightness as a function of air mass on a typical day. The intercept for zero air mass provides the calibration of the instrument intensity signal for that day.

From a plot of the intercept value as a function of date, the intensity changes resulting from phototube voltage changes were found. The calibrated disk average intensity from the magnetograms is plotted in Figure 3. Most of the variation with time is due to the varying amount of dirt on the optics. The arrows show the times that the coelostat mirror and lenses were cleaned.

c) *Velocity Calibration and Corrections*

The velocity observations are made by measuring the position of the spectral line. The spectrograph exit aperture consists of a pair of prisms mounted such that each prism gets light from one wing of the line and directs it to a photomultiplier tube. The prism assembly is mounted on accurate ways and positioned by a precise measuring screw. A shaft encoder is used to record the position of the prisms while a servo system keeps them centered on the line. One count of the encoder corresponds to 1/4096 of a turn of the screw with 10 turns per inch. Thus, for the dispersion at 5250 Å, the velocity calibration is 2.752 m s^{-1} per encoder count. This corresponds to about 0.6 μm of physical displacement of the prisms and is about the practical limit for a mechanical measuring engine. The rms variation due to spectrograph seeing, electronic noise, and servo errors is typically 10 m s^{-1} for a 15 s observation in integrated light. The velocity calibration is measured each day as part of a series of automatic checks; however, since the uncertainty in the daily measurement of dispersion is larger than the variations, a constant value is used for the data reported here.

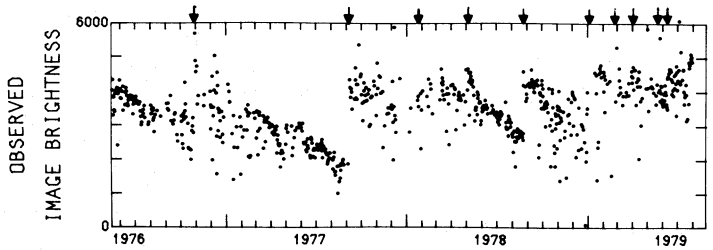

FIG. 3.—Observed image brightness for each magnetogram through 1979 July. The arrows show the dates on which the optics were cleaned. Intensity changes due to other instrument changes have been removed.

Before the observed line position data can be interpreted as motions of the Sun, the relative motion of the observatory and the Sun must be removed and spectrograph drifts must be removed. The Doppler shifts resulting from the Earth's rotation and orbital motion are removed for each point observed using the method described by Howard and Harvey (1970) and Howard, Boyden, and LaBonte (1980).

Other sources of drift in the velocity data include a slow motion of the diffraction grating during the first hour after it is repositioned, changes in the index of refraction of the air in the spectrograph, and drifts in the relative gain of the phototubes. To reduce the effect of the grating drift, the start of each scan is delayed for about a half-hour after the grating is positioned. In order to remove the remaining drifts from the data, a pair of 5 minute integrations is made at the center of the disk, one before and one after the scan. It is assumed that the drifts are linear in time, and these two disk-center averages are used to define the zero line. Figure 4 shows the total amount of this drift for each of the observations used for this study.

Once the relative motions and drifts are removed, the rotation rate of the photosphere can be computed. The first question one must address when measuring solar rotation is how to describe that rotation. The traditional method has been to assume that the antisymmetrical part of the Dopplergram can be described by a relation of the form:

$$\omega = a + b\sin^2 B + c\sin^4 B + \text{other terms}, \qquad (1)$$

where ω is the angular velocity, B is the heliographic latitude, and a, b, and c are to be found from a least-squares or other fit to the data (e.g., Howard and Harvey 1970). We use the same general method with a few differences. Since the observed quantity is a line-of-sight velocity and some of the systematic errors are shifts in apparent wavelength, we choose to express the determined coefficients and thus the rotation rate in m s^{-1} rather that rad s^{-1}. This necessitates conversion of the final result to angular velocity for comparisons but is more convenient for studying the various systematic effects. The limb redshift is assumed to be symmetrical about central meridian so that it will not affect the rotation-rate terms and is not explicitly removed. The magnitude of the limb shift is expected to be about 30 m s^{-1} at the boundary of the 0.75 $R_\odot$ disk used for the rotation studies and will be discussed in a future paper. Since an error in the computed position angle of the solar pole will produce an apparent north-south velocity at the expense of rotation, the linear antisymmetrical part of the velocity in the north-south direction is also found.

The form for differential rotation used is the same as used by Howard and Harvey (1970), but we make the assumption that the terms b and c in (1) have the same value. There is a computational problem resulting from the nonorthogonality of the terms used to describe rotation (Duvall and Svalgaard 1978; Stenflo 1977). The effect of this is that noise in the data will shift the amplitude between the b and c terms. Since the time-averaged values of b and c are about the same when (1) is used to determine rotation, it is assumed here that $b=c$. Any errors resulting from this assumption will appear as stable features in the residuals and will be examined in a later paper. In any case, the assumed equality of b and c has a negligible effect on the a coefficient.

Since the observed quantity is the line-of-sight component of velocity, and since rotation results in a purely azimuthal motion, the correction factor $\cos B \cos B_0 \sin L$ is used, where B_0 is the heliographic latitude of the disk center and L is the heliographic longitude measured from disk center. Thus the relation used to express rotation has the form:

$$V = \left[e + b\sin^2 B(1+\sin^2 B) \right] \times \cos B \cos B_0 \sin L + p \sin B. \qquad (2)$$

The coefficients e, b, and p in (2) are found for each scan by the method of least squares with each of the data values weighted by the intensity corrected for limb darkening. This weighting helps ensure that an occasional cloud will not adversely affect the results. Once

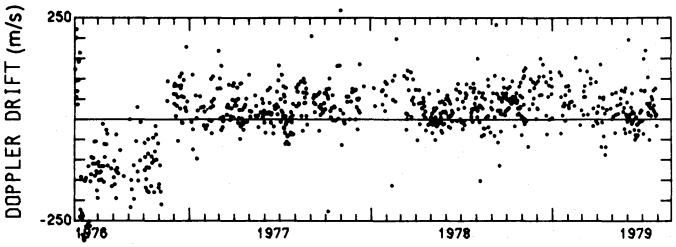

FIG. 4.—Drift in the velocity signal ascribed to spectrograph and electronics drifts. The total amount of the drift between the reference integrations is shown. The average magnitude of the drift was 43 m s^{-1} hr^{-1}. The algorithm for positioning the grating was changed in 1976 October to reduce the residual grating motion.

the coefficients above have been found, the error in the position angle can be found from

$$p_{\rm err} = \tan^{-1}(p/e),$$

and the equatorial rotation velocity is found from

$$a = \sqrt{e^2 + p^2}\ .$$

In practice, $p_{\rm err}$ has been found to be small with a typical value of 0°.1. In addition to the terms a, b, and $p_{\rm err}$ found above, a term a_0 is found from a second fit to the data with the term b replaced with a constant -300 m s^{-1}. The coefficients a_0, a, and b have been found for all reasonable completed scans to date. Of the total 975 scans 244 were eliminated because they were incomplete or were made during such bad weather the data were obviously not useful.

In addition to the above corrections, there are two types of systematic effect that should be considered for the SSO instrument. These are the alignment of the entrance slit and the exit slit and the presence of significant amounts of scattered light for the earlier observations. (We now keep the optics scrupulously clean so that scattered light is of the order of one part in a thousand.)

The combined effect of the use of an image slicer, a 3′ aperture, and the north-south direction of the entrance slit results in a signal in the same sense as solar rotation if the exit slit is not exactly parallel to the entrance slit. Prior to 1978 February 15 there was a small misalignment that caused such an error (as described by Duvall 1979). In addition to altering the observed rotation rate, the misalignment of the slits results in an apparent change in rotation with distance from disk center. The net effect can be clearly seen by comparing uncorrected Dopplergrams for observations before and after the slit readjustment. Figure 5 shows two such Dopplergrams. The closed contours at the east and west limbs in Figure 5*a* are the result of the misalignment. An analysis of the correlation between the equatorial rotation rate and intensity (as described below) shows that the data before the slits were properly adjusted should be increased by 2.1%. This correction has been included in the results presented here.

III. EFFECT OF SCATTERED LIGHT

a) The Problem

Figure 6 shows the observed equatorial rate a_0 corrected for all the effects described above. The general character of the data is a sequence of slow declines followed by sudden increases. The arrows show the times that the coelostat mirror was removed and cleaned or resurfaced. There is a clear connection between the times of cleaning and the times of sharp increase in observed rotation rate. The correlation between the observed brightness shown in Figures 3 and 6 is also obvious. After each cleaning of the optics, the intensity and a_0 both jump. As dust and smog accumulate on the mirrors and lens, both the intensity of the image and the observed rotation rate decrease. This correlation is to be expected since as the dust scatters light out of the main beam, it mixes light from the entire disk with light from a particular region.

The details of the expected effect depend on the density of scattering sources, the size and height distribution of the particles, and the angular aperture of the instrument. In any case it is expected that the effect on the rotation rate will be proportional to the scattered brightness just off the limb. Because of the limited angular aperture the effective intensity of the scattered light will be proportional to the density of scatterers while the direct intensity will decrease exponentially with the number of scatterers. Therefore, in the analysis below, the natural logarithm of the intensity is used for comparison to the rotation rate. The

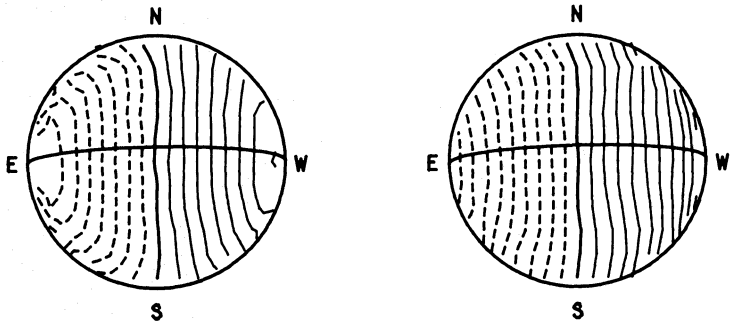

FIG. 5.—Solar velocity contours as observed. Dashed contours are motion toward the observer, solid away. The contour interval is 200 m s^{-1}. A solid-body rotation would result in straight vertical contours. Data for two days is shown: (*a*) (1978 February 15) observed with an entrance slit alignment error that affects velocity measurements near the limb; (*b*) (1978 March 16) typical for observations with the correct alignment.

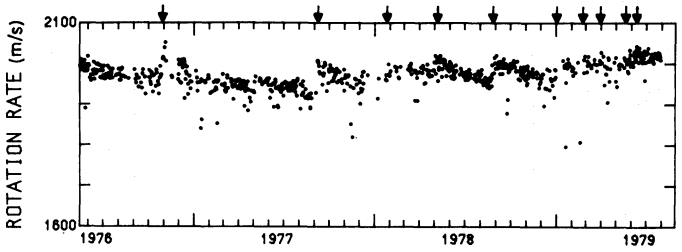

FIG. 6.—Solar equatorial rotation rate a_0 for each magnetogram scan included in this analysis. There are tick marks at the first of each month. The arrows show the dates of cleaning and realuminizing the mirrors.

effect of scattered light from the instrument and the sky on rotation measurements has been known for a long time (e.g., Plaskett 1915).

b) *The Correction*

Since there is an effect on the observed velocities due to scattered light, observation should only be made with clear skies and clean optics. In the past at the SSO this condition was not always met, but since the observations made in less than optimum conditions contain a significant amount of information about solar motions, we have attempted to remove as much of the effect of scattered light as possible. This is done by finding an empirical relation between the intensity I and a_0. We expect

$$I = I_0 e^{-T},$$

where T is the optical thickness. The scattered light intensity S off the limb (as a fraction of the disk center intensity) should be proportional to T, so we can write

$$I = I_0 e^{-kS}. \tag{3}$$

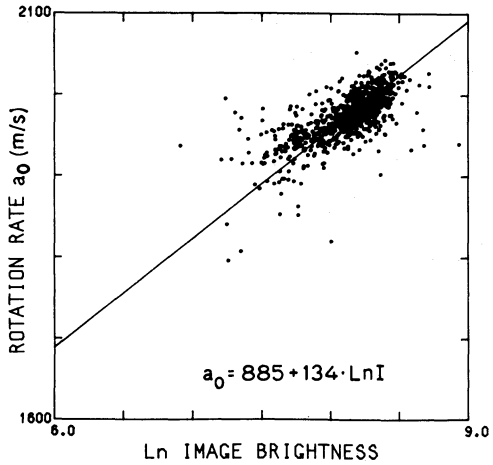

FIG. 7.—A scatterplot of the equatorial rotation rate a_0 as a function of the logarithm of the observed image brightness $\ln(I)$. The best-fit line shown is used to determine the error in a_0 which is due to the correlation with intensity.

The decrease in observed rotational velocity should be proportional to S, so we can write

$$V_{\mathrm{obs}} = V_{\mathrm{actual}} - \alpha S, \tag{4}$$

then combining (3) and (4) we expect

$$V_{\mathrm{obs}} = V_{\mathrm{actual}} - \alpha/k\ (\ln I_0 - \ln I). \tag{5}$$

Since V_{obs} and $\ln I$ are observed, α/k and $\ln I_0$ are needed to find V_{actual}. Figure 7 shows a scatterplot of V_{obs} and $\ln I$. The line is the least-squares linear regression line $V = 134 \ln I + 885$. A separate analysis for data before and after 1978 February 15 yielded the 2.1% correction to compensate for the slit adjustment described above.

To complete the correction we need to know I_0, that is, the intensity (corrected for phototube changes) that would have been found with clean sky and optics. Since 1978 August the scattered light intensity just off the limb has been measured at the start of each scan. Figure 8*a* shows $\ln I$ versus S. The intercept of the best-fit line yields $\ln I_0 = 8.56$. Thus we have

$$V_{\mathrm{corrected}} = V_{\mathrm{obs}} + 134(8.56 - \ln I). \tag{6}$$

Figure 8*b* shows the correlation between the observed rotation velocity and the measured scattered light. The roughly linear relationship here justifies the form of equation (4). The slope of the line in Figure 8*b* is the term α in equation (4), and similarly Figure 8*a* provides directly a value for k in equation (3). These combine to yield $\alpha/k = 119$ which is in close agreement with the value for α/k derived from the direct comparison of intensity and rotation in Figure 7. Owing to uncertainties in assessing the relative errors in the computed rotation rate and the observed scattered light, the slopes of the lines in Figures 8*a* and 8*b* have poorly determined errors. The expected maximum value for the slope in Figure 8*b* is about 20 m s^{-1} per percent scattered light. Inspection of Figure 8 shows that a smaller value of the slopes of the lines is consistent with the data, with the expected value of 20 m s^{-1} per percent scattered light, and with the ratio α/k found in Figure 7.

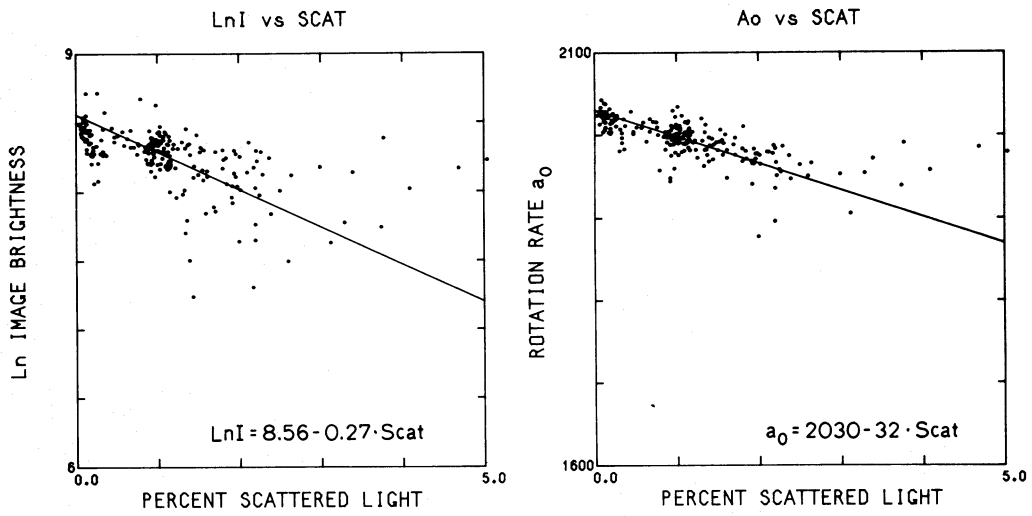

FIG. 8.—Scatterplots of (*a*) ln(*I*) and (*b*) a_0 with the observed scattered light *S* for those observations for which *S* was measured. The quantity *S* is the brightness in the 3′ aperture centered about 2′ off the limb relative to the disk center brightness. The intercept in Fig. 8*a* shows the brightness with no scattered light I_0, while the slope of the best-fit lines in Figs. 8*a* and 8*b* verify the correction factor derived in Fig. 7.

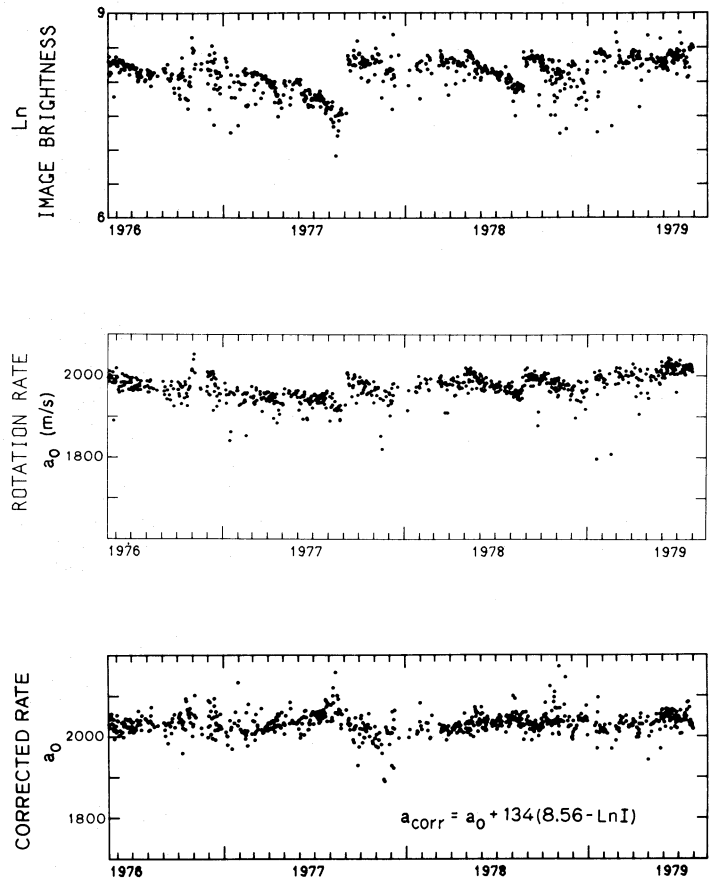

FIG. 9.—(*a*) The observed image brightness (from Fig. 3); (*b*) the observed rotation rate a_0 (from Fig. 6); and (*c*) the corrected equatorial rotation rate for all included scans. The correction was applied separately for each scan; thus some of the variance in brightness which is not correlated with scattered light tends to increase the variance in the corrected rotation rate. The estimate for day-to-day variations in a_0 is made from Fig. 9*b* disregarding the drift resulting from the correlation with 9*a*.

IV. DISCUSSION

a) *The Variability of Solar Rotation*

Figure 9*c* shows the equatorial rotation rate a_0 as corrected with relation (6). Figure 9*a* is the logarithm of the brightness data from Figure 3, and Figure 9*b* is the data from Figure 6 shown here for comparison. Several statements concerning the nature of solar rotation can be made by examining these data. The first and most certain is that the day-to-day variation in the observed value is small with an rms variation from the mean of 26 m s^{-1} or about 1.3%. During intervals of good weather, as indicated by small variance in the intensity, it can be seen that the solar contribution to the observed velocity variations is probably smaller than 20 m s^{-1}. These relatively small upper limits for the short-term fluctuations in solar rotation are noticeably smaller than the values previously reported for Doppler-shift–type observations.

Examination of Figure 9 also shows that there are no identifiable seasonal or yearly variations during the 3 years of available data that exceed 20 m s^{-1}. This can be confirmed from Figure 10 which is the result of a 108 day low-pass filtering of Figure 9*c*. Considering the uncertainties in the corrections applied, there is no justification for concluding that even these small variations are of solar origin. There may, of course, be long-term variations in the rotation rate that are masked by uncertainties in the corrections. While variations larger than 1% seem to be excluded by this analysis, a 1% increase in 3 years (as suggested by Howard 1976*b* and by Livingston and Duvall 1979) could have been masked by an error in the slit alignment correction.

b) *Actual Value of Solar Rotation*

Newton and Nunn (1951) reported the average rotation rate of long-lived recurrent sunspots. Using their form for differential rotation, the equatorial rate from sunspot observations is 2020 m s^{-1}. An inspection of Figure 9 shows that, to the certainty of the corrections, the photospheric material also rotates at this rate. Considering the possible uncertainty in the corrections it is worthwhile to examine separately the data since 1979

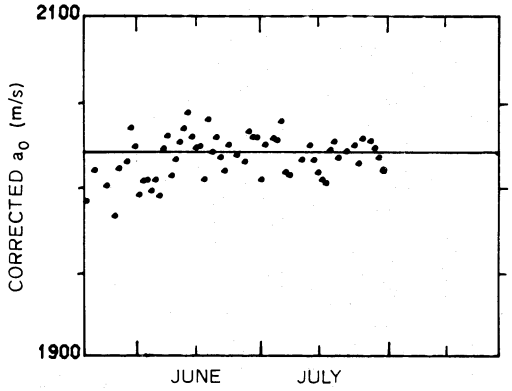

FIG. 11.—The observed (uncorrected) equatorial rate for the most recent data (clean optics). The horizontal line is drawn at the Newton and Nunn rate of 2020 m s^{-1}. The simple mean of the data shown is 2016 m s^{-1} with a standard deviation of 13 m s^{-1}.

May 18. While this represents only 60 observations, the scattered light has been low enough that no correction is necessary. Figure 11 shows this data. There has been no change in the procedure during this time except to keep the optics clean to exclude an effect from scattered light. The average value of the uncorrected rate a_0 for this interval is 2016 ± 13 m s^{-1}. In order to be fully confident of the constancy of this value, an additional year or more of observations must be made, but it is safe to say that in 1979 June the photospheric material rotated at the Newton and Nunn rate.

V. CONCLUSIONS

Several points need to be reviewed. At the SSO, measurements of the solar rotation rate have been made since 1976 May. In the earlier observations, the measured velocities were contaminated by scattered light. This is exhibited by an obvious correlation between the observed intensity and velocity data. When the effect of scattered light is removed by empirical methods it is found that (*a*) the day-to-day variations in the equatorial rotation are at most 20 m s^{-1} rms about the mean; (*b*) there are no long-term trends exceeding 1% that can be associated with the Sun rather than the instrument; and (*c*) the average rate

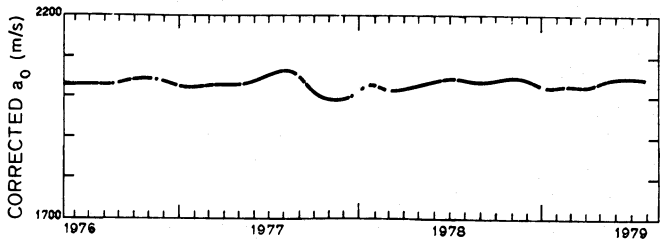

FIG. 10.—Slow drifts in the corrected equatorial rate. A 108 day low pass filter has been applied. The trends in this figure are probably due to the incomplete removal of instrumental problems.

for the photosphere is most likely about the same as the Newton and Nunn rate for sunspots. Point (*b*) is not yet in conflict with the results of Howard (1976*b*) and Livingston and Duvall (1979).

It was also found that the fewer the number of terms used to express solar rotation the smaller the variance in the rate determined. When the term for differential rotation is also fitted to the data the rotation is found to be:

$$V = 2030 - 278 \sin^2 B - 278 \sin^4 B \text{ m s}^{-1}$$

(at one solar radius), which is the same as

$$\omega = 2.917 - 0.40 \sin^2 B - 0.40 \sin^4 B \ \mu\text{rad s}^{-1}.$$

These conclusions are different from the commonly held belief that the photosphere in general rotates slower than large-scale magnetic field structures and that the rate shows substantial variations. It is unlikely that magnetograph-type observations made at other observatories suffer from the specific errors that formerly existed at the SSO (e.g., scattered light), but there may be some as yet unidentified sources of instrumental noise. If there is some noise which is not purely random then the observations may not be in conflict, but only the interpretations.

This work was assisted by discussions at the Workshop on Solar Rotation Observations held at Hale Observatories in 1979 March. This work was supported in part by the Office of Naval Research under Contract N00014-76-C-0207, by the National Aeronautics and Space Administration under grant NGR 05-020-559 and contract NAS5-24420, and by the Division of Atmospheric Sciences, Solar Terrestrial Research Program of the National Science Foundation under grant ATM77-20580.

REFERENCES

DeLury, R. E. 1939, *J.R.A.S. Canada*, **33**, 345.
Duvall, T. L., Jr. 1979, *Solar Phys.*, **63**, 3.
Duvall, T. L., Jr., and Svalgaard, L. 1978, *Solar Phys.*, **56**, 463.
Hart, A. B. 1954, *M.N.R.A.S.*, **114**, 2.
Howard, R. 1976*a*, *Solar Phys.*, **48**, 411.
_____. 1976*b*, *Ap. J. (Letters)*, **210**, L159.
_____. 1978, *Rev. Geophys. Space Phys.*, **16**, 721.
Howard, R., Boyden, J. E., and LaBonte, B. J. 1980, *Solar Phys.*, in press.
Howard, R., and Harvey, J. 1970, *Solar Phys.*, **12**, 23.
Howard, R., Tanenbaum, A. S., and Wilcox, J. M. 1968, *Solar Phys.*, **4**, 286.
Livingston, W., and Duvall, T. L., Jr. 1979, *Solar Phys.*, **61**, 219.
Newton, H. W., and Nunn, M. L. 1951, *M.N.R.A.S.*, **111**, 413.
Plaskett, H. H. 1973, *M.N.R.A.S.*, **163**, 183.
Plaskett, J. S. 1915, *Ap. J.*, **42**, 373.
Scherrer, P. H., Wilcox, J. M., Svalgaard, L., Duvall, T. L., Jr., Dittmer, P. H., and Gustafson, E. K. 1977, *Solar Phys.*, **54**, 353.
Stenflo, J. O. 1977, *Astr. Ap.*, **61**, 797.
Svalgaard, L., Scherrer, P. H., and Wilcox, J. M. 1979, *Proc. Workshop on Solar Rotation*, ed. G. Belvedere and L. Paterno, Osservatorio Astrofisico di Catania, Publicazione No. 162, 151.

P. H. SCHERRER and J. M. WILCOX: Institute for Plasma Research, Stanford University, Via Crespi, Stanford, CA 94305

L. SVALGAARD: Université de Liège, Institut d'Astrophysique, Cointe-Ougrée, Belgium